Role of APOA1 in the Resistance to Platinum-Based Chemotherapy in Squamous Cervical Cancer

Yue He
Capital Medical University Beijing Obstetrics and Gynecology Hospital
Su-Bin Han
Capital Medical University Beijing Obstetrics and Gynecology Hospital
Yang Liu
Capital Medical University Beijing Obstetrics and Gynecology Hospital
Jing-Jing Zhang
Capital Medical University Beijing Obstetrics and Gynecology Hospital
Yu-Mei Wu (wym597118@ccmu.edu.cn)
Capital Medical University Beijing Obstetrics and Gynecology Hospital

Research

Keywords: Cervical cancer, chemotherapy resistance, apolipoprotein A1, platinum, proteomics

Posted Date: June 7th, 2021

DOI: https://doi.org/10.21203/rs.3.rs-544694/v1

Version of Record: A version of this preprint was published at BMC Cancer on April 14th, 2022. See the published version at https://doi.org/10.1186/s12885-022-09528-x.

Abstract

Introduction: To investigate the mechanism by which apolipoprotein A1 (APOA1) enhances the resistance of cervical squamous carcinoma to platinum-based chemotherapy.

Methods: Two cervical squamous carcinoma cell lines (SiHa and Caski) overexpressing APOA1 (OE) were constructed, treated with carboplatin (CBP), and compared to normal control (NC) cells.

Results: In both cell lines, the clone-forming ability of CBP-treated cells was lower than that of untreated cells, and the clone formation rate of OE cells was lower than that of NC cells ($p < 0.05$), indicating that APOA1 overexpression enhanced chemoresistance. A screen for APOA1 downstream proteins affecting platinum-based chemoresistance using TMT revealed 64 differentially expressed proteins, which were subjected to GO annotation, KEGG enrichment, subcellular localization, structural domain annotation and enrichment, clustering, and interaction network analyses. Twenty-nine differentially expressed proteins matching cancer-relavent association terms were screened and parallel response monitoring identified 21 as possibly involved in the mechanism of platinum-based chemoresistance.

Conclusions: Our analysis suggested that the mechanism may involve numerous regulatory pathways, including promoting tumor growth via the P38 MAPK signaling pathway through STAT1, promoting tumor progression via the PI3K signaling pathway through CD81 and C3, and promoting resistance to platinum-based chemotherapy resistance through TOP2A.

Introduction

Cervical cancer is a common malignant tumor of the female reproductive system. One of the main treatments for advanced and recurrent cervical cancer is chemotherapy, and platinum-based regimens are first-line chemotherapeutics [1]. Resistance to chemotherapy is a key factor affecting treatment outcomes for advanced and recurrent cervical cancer.

Apolipoprotein A1 (APOA1) is the main structural protein in high-density lipoprotein (HDL), mainly involved in reverse cholesterol transport. Several studies have found that APOA1 plays important roles in tumor growth, angiogenesis, and invasion, and metastasis [2]. Although a few studies on APOA1 and tumor chemotherapy have been reported, the mechanism underlying the role of APOA1 in platinum-based chemotherapy resistance in cervical cancer has not been reported. We previously constructed cervical cancer SiHa cell lines stably overexpressing the *APOA1* gene using a lentiviral vector [3] and demonstrated that APOA1 is a cervical cancer drug resistance-associated protein involved in resistance to chemotherapy, especially platinum-based chemotherapy, in cervical cancer [4]. The present study aimed to further explore the function and mechanism of APOA1 in platinum-based chemoresistance in cervical cancer.

Materials And Methods

Materials

Human cervical squamous carcinoma cell lines (SiHa and Caski) were obtained from the Laboratory of the School of Basic Medical Sciences, Capital Medical University (Beijing, China). The following materials were used in this study: DMEM (HyClone,Utah，USA), fetal bovine serum (Four Seasons Green, Hangzhou, China), carboplatin (CBP) (CST，Boston，USA), Triton X-100 (Sigma，St. Louis，USA), TMR red (Roche，Basel, Switzerland), Transwell kit (Corning，New York，USA), GIEMSA staining solution (Sigma，St. Louis，USA) and MTT，Genview，Genview，USA).

Methods

Cell culture. APOA1-overexpression (OE) and control lentivirus-transfected (negative control, NC) SiHa and Caski cells were cultured in DMEM containing 10% fetal bovine serum at 37℃ in a 5% CO_2 incubator. The medium was changed every 2–3 days, and cells in logarithmic growth phase were used in the experiments.

Clone formation assay. SiHa and Caski OE and NC cells were collected, trypsinized, and counted; then, the cell suspensions were diluted and inoculated into 6-well plates at a concentration of 500 cells per well. The cells were cultured in a cell culture incubator for 14 days, until visible cell clones appeared. Clones were counted with the naked eye, and the number of clones with > 50 cells were counted under a microscope. The clone formation rate was calculated using the following formula: Clone formation rate = (number of clones/number of inoculated cells) × 100%.

MTT assay. SiHa and Caski OE and NC cells were collected, trypsinized, and counted. The density of the cell suspensions was adjusted to 2×10^3 cells/ml, and the cells were inoculated into 96-well plates and incubated for 1, 2, 3, 4, and 5 days. After incubation, the medium was discarded, and 20 μL of MTT (5 mg/mL) was added to each well. Then, 100 μL of DMSO was added to dissolve the formazan crystals, and the OD at 490 nm was measured with a microplate reader. Finally, the relative cell viability was calculated based on the OD, and a growth curve was generated.

TUNEL assay. SiHa and Caski OE and NC cells were collected, trypsinized, and counted. The cells were then washed, placed in complete medium containing carboplatin (CBP), and incubated for 48 h. Cells were fixed with 4% paraformaldehyde in PBS solution (pH 7.4) at 15–25°C for 1 h and then washed with PBS. Cells were permeabilized using a sodium citrate solution containing 0.1% Triton X-100 and incubated in an ice bath (2–8°C) for 2 min. Then, 50 μl of prepared DNase I was added, and the cells were incubated at 20°C for 10 min. TUNEL reaction mix was prepared by mixing 50 μl of TdT with 450 μl of fluorescein-labeled dUTP solution. The prepared TUNEL reaction mix (50 μl) was added to each specimen, which was incubated at 37°C for 1 h. The negative control contained fluorescein-labeled dUTP solution only. Nuclei were stained with 50 μl of 5 μg/ml DAPI for 5 min at 20℃ and rinsed thrice in PBS. Finally, TUNEL and DAPI-labeled cells were counted separately under a fluorescence microscope.

Tandem Mass Tag (TMT) screening of ApoA1 downstream related proteins. The samples were labeled with isotopes. Biological analyses included GO term analysis, KEGG pathway annotation and enrichment analysis, subcellular localization analysis, domain annotation and enrichment analysis, and clustering and interaction network analysis. Proteins that met the screening criteria, i.e., expression > 1.2 times higher or lower and a p value less than 0.05 by *t*-test, were regarded as differentially expressed proteins. The IPA bioinformatics analysis was performed using the following keywords: JAK stat, Notch signaling, p38 MAPK signaling, PI3K signaling, tumor progression, chemotherapy, recurrence, drug resistance, and metastasis.

Protein sampling and electrophoresis. Cell lysate samples were mixed with SDT buffer (4% SDS, 100 mM DTT, 150 mM Tris-HCl, pH 8.0), sonicated, and then boiled for 15 min. After centrifugation at 14000 × *g* for 40 min, the protein concentration in the supernatant was quantified using the BCA Protein Assay Kit (P0012; Beyotime,Shanghai□China). The sample was stored at -20°C until use.

Filter-aided sample preparation (FASP). Samples containing 200 μg of protein were mixed with 30 μl of SDT buffer. Then, the detergent, DTT, and other low-molecular-weight components were removed by repeated ultrafiltration (30 kDa; Sartorius) into UA buffer (8 M Urea, 150 mM Tris-HCl, pH 8.5). Then, 100 μl of iodoacetamide (100 mM in UA buffer) was added to block reduced cysteine residues, and the samples were incubated for 30 min in the dark. The filters were washed thrice with 100 μl of UA buffer and then twice with 100 μl of 0.1 M TEAB buffer. Finally, the proteins were digested with 4 μg of trypsin (Promega,Madison□USA) in 40 μl of 0.1 M TEAB buffer overnight at 37°C, and the resulting peptides were collected as a filtrate. The peptide content was estimated by measuring UV light spectral density at 280 nm using an extinction coefficient of 1.1 in a 0.1% (g/l) solution, which was calculated based on the frequency of tryptophan and tyrosine residues in vertebrate proteins.

TMT Labeling. An aliquot of each sample (containing 100 μg of peptides) was labeled with TMT reagent according to the manufacturer's instructions (Thermo Fisher Scientific, Waltham, USA).

Peptide fractionation using reversed phase (RP) chromatography. TMT-labeled peptides were fractionated by RP chromatography using an Agilent 1260 Infinity II HPLC system. The peptide mixture was diluted with buffer A (10 mM $HCOONH_4$, 5% ACN, pH 10.0) and loaded onto a XBridge Peptide BEH C18 Column (130 Å, 5 μm, 4.6 mm × 100 mm). The peptides were eluted at a flow rate of 1 ml/min with a gradient of 0–7% buffer B (10 mM $HCOONH_4$, 85% ACN, pH 10.0) for 5 min, 7–40% buffer B from 5 to 40 min, 40–100% buffer B from 45 to 50 min, and 100% buffer B for 50 to 65 min. Elution was monitored at 214 nm based on the UV light trace, and fractions were collected every 1 min from 5 to 50 min. The collected fractions were combined into 10 fractions and dried via vacuum centrifugation at 45°C.

Easy nLC mass spectrometry analysis. Each fraction was subjected to nanoLC-MS/MS analysis. Each peptide mixture was loaded onto a C18-reversed phase analytical column (Acclaim PepMap RSLC 50 μm × 15 cm, nano viper, P/N164943; Thermo Fisher Scientific) in buffer A (0.1% formic acid) and separated with a linear gradient of buffer B (80% acetonitrile and 0.1% formic acid) at a flow rate of 300 nl/min: 6%

buffer B for 3 min, 6–28% buffer B for 42 min, 28–38% buffer B for 5 min, 38–100% buffer B for 5 min, and 100% buffer B for 5 min.

Data analysis. MS/MS raw files were processed using the MASCOT engine (version 2.6; Matrix Science, London, UK) in Proteome Discoverer 2.2 and searched against the database *Uniprot_HomoSapiens_20367_20200226*. The search parameters included trypsin as the enzyme used to generate peptides and a maximum of two missed cleavages. A precursor mass tolerance of 10 ppm was specified as well as a 0.05 Da tolerance for MS2 fragments. Except for TMT labels, carbamidomethyl (C) was set as a fixed modification. Variable modifications were Oxidation (M) and Acetyl (Protein N-term). A peptide and protein false discovery rate of 1% was enforced using a reverse database search strategy. Proteins with a fold change greater than 1.2 and a p value less than 0.05 (Student's *t*-test) were considered differentially expressed.

Bioinformatics analyses

Gene Ontology (GO) annotation. First, all protein sequences were aligned to a database downloaded from NCBI (ncbi-blast-2.2.28+-win32.exe), and only the top 10 sequences with an E-value $\leq 1\times10^{-3}$ were included in the analysis. Second, the GO term (database version: go_201504.obo) for the sequence with the top Bit-Score as determined by Blast2GO was selected. Then, the annotation from the GO terms for the proteins was completed using Blast2GO Command Line. After simple annotation, InterProScan was used to search the EBI database by motif, and the functional information for the motifs was added to the proteins to improve the annotation. Next, the annotation and connections between GO terms were further improved using ANNEX. Fisher's exact test was used to enrich GO terms by comparing the number of differentially expressed proteins and total proteins correlated to the GO terms.

KEGG annotation. Pathway analysis was performed using the KEGG database. Fisher's exact test was used to identify the significantly enriched pathways by comparing the number of differentially expressed proteins and total proteins in each pathway.

Subcellular localization analysis. We used Wolf PSORT to predict the location of different proteins. Wolf PSORT is a tool that is commonly used to predict the subcellular localization of proteins (https://wolfpsort.hgc.jp/). The program transforms protein sequences into digital location features based on sorting signals, the amino acid composition, and functional motifs. Then, the k-nearest neighbor classifier is used to predict their subcellular localization.

Domain annotation and enrichment analysis. The InterPro database integrates the functions of protein sequence family classification with domain and special site prediction. We used this database to annotate the functional domains of proteins of interest. Fisher's exact test was used to compare the distribution of different proteins in the total protein set to evaluate the significance of the enrichment of a specific functional domain.

Clustering. For the first step of cluster analysis, the quantitative information for the target protein set was normalized. Then, Matplotlib was used to classify the two dimensions of sample and protein expression

(distance algorithm: Euclidean, connection method: average link). Finally, a hierarchical clustering heat map was generated.

Protein-protein interaction network. To analyze the PPI networks, the gene symbols of the target protein were obtained from the database containing the target protein sequences, and these gene symbols were used in intAct (http://www.ebi.ac.uk/intact/main.xhtml). The direct and indirect interactions between the target proteins were found in the database. The interaction network was generated and analyzed using Cytoscape software (version: 3.2.1)

Analysis of IPA-related words. The IPA analysis was performed with the following keywords as input: JAK stat, Notch signaling, p38 MAPK signaling, PI3K signaling, tumor progression, chemotherapy, recurrence, drug resistance, and metastasis.

Identification of AOPA1 downstream proteins by PRM.

Ion screening of PRM peptides. Using Proteome Discoverer 2.1 (Thermo Fisher Scientific) software, the original spectrum file (.Raw file) generated by Q Exactive was transformed into an MGF file, which was submitted to the Mascot 2.6 server for database retrieval using the built-in tool of the software. The database used was *UniProt_HomoSapiens_20367_20200226* (http://www.uniprot.org). Based on the results of the analysis, the unique peptides of the target proteins were screened, and information, such as the mass charge ratio, number of charges, and retention time, were obtained and imported into the inclusion list.

Quantitative identification of PRM. Mass spectrometry was performed using an Easy nLC according to the manufacturer's instructions. The mass spectrum parameters were as follows: for Full-MS. scan range (m/z) 350–1800, resolution = 70,000, AGC target = 3e6, maximum injection time = 50 ms; for PRM, resolution = 17,500, AGC target = 2e5, maximum injection time = 45 ms, Loop count = 10, Isolation window = 2 m/z, and NCE = 27%.

Statistical methods. SPSS 20.0 was used for all statistical analyses and for generating graphics. Measurement data were expressed as mean ± standard deviation (x ± s). Statistical *t*-test was used to compare the means between two groups, ANOVA was used to compare the means among multiple groups, and the chi square test was used to compare rates between groups, A p value less than 0.05 was considered statistically significant.

Results

Effects of APOA1 overexpression on cervical squamous carcinoma cells after carboplatin treatment

Effect on clone formation ability. To investigate the effect of APOA1 overexpression on the clone formation ability of cervical squamous carcinoma SiHa and Caski cells treated with carboplatin, the

colony forming ability of both normal cells (NC) and cells overexpressing APOA1 (OE) was observed in the presence and absence of carboplatin using a plate colony assay. Cells were treated with carboplatin for 48 h, and the number of colonies was counted after 12 days of incubation. The results showed that in Caski cells, the number of clones was 85 ± 5 in the NC group, 68 ± 5 in the OE group, 9 ± 2 in the NC + carboplatin group, and 21 ± 4 in the OE + carboplatin group. The change in the clone formation rate following administration of chemotherapy was smaller in the OE groups than in the NC groups ($p < 0.05$). In SiHa cells, the number of clones was 47 ± 6 in the NC group, 33 ± 4 in the OE group, 13 ± 4 in the NC + carboplatin group, and 15 ± 2 in the OE + carboplatin group. The change in clone formation rate following administration of chemotherapy was smaller in the OE group than in the NC group ($p < 0.05$) (Fig. 1).

Effect on cell proliferation. To investigate the effect of APOA1 overexpression on the proliferation of cervical squamous carcinoma SiHa and Caski cells, NC and OE cells were incubated for 1–5 days and then treated with carboplatin (30 μg/ml) for 48 h. Relative cell viability was measured by the MTT assay. The results showed that the difference in cell proliferation between NC and OE cells was not statistically significant, with or without carboplatin ($p > 0.05$) (Fig. 2).

Effect on apoptosis. To investigate the effect of APOA1 overexpression on the apoptosis of SiHa and Caski cells induced by carboplatin, NC and OE cells were treated with CBP (30 μg/ml) for 48 h. Then, apoptosis was assessed by the TUNEL method. The results are shown in Fig. 3.

Apoptosis rate in SiHa cells Apoptosis rate in Caski cells

Screen for differentially expressed proteins downstream of APOA1 that involved in platinum-based chemoresistance and bioinformatics analysis.

Proteins were labeled using TMT and analyzed using tandem mass spectrometry (MS/MS). The obtained data were subjected to significant difference analysis, GO annotation and enrichment analysis, KEGG pathway annotation and enrichment analysis, subcellular localization analysis, structural domain annotation and enrichment analysis, clustering analysis, and interaction network analysis. After cleavage, a total of 5983 proteins were detected and included in the analyses for differentially expressed proteins downstream of APOA1.

Analysis of differentially expressed proteins. In the screening for differentially expressed proteins, the criteria were a greater than 1.2-fold difference in expression (for upregulated and downregulated proteins) and a p value less than 0.05 as determined by t-test. In the CBP-treated groups, there were 64 differentially expressed proteins between OE and NC cells; 35 were upregulated, and 29 were downregulated (Table 1).

Table 1
TMT screening of differentially expressed proteins downstream of APOA1 involved in platinum-based chemotherapy resistance

Comparison	Upregulated	Downregulated	Total
OE vs. NC	16	5	21
NC + CBP vs. NC	13	12	25
OE + CBP vs. OE	32	68	100
OE + CBP vs. NC + CBP	**35**	**29**	**64**

Comparisons: groups included in the protein expression comparisons: Upregulated, upregulated proteins; Downregulated, downregulated proteins; Total, all differentially expressed proteins

GO enrichment analysis. Using GO enrichment analysis, the target proteins were classified according to biological process, molecular function, and the cellular components they reside in. The distribution of differentially expressed proteins in OE + CBP compared to NC + CBP according to each classification is shown in Fig. 4.

KEGG pathway enrichment analysis. The method used for the KEGG pathway enrichment analysis is similar to that of the GO enrichment analysis, in that the KEGG pathway was used as a unit and all qualitative proteins were used as the background. To identify significantly affected metabolic and signaling pathways, the significance of protein enrichment in each pathway was calculated using Fisher's exact test. The OE + CBP and NC + CBP groups were compared to analyze which pathways the differentially expressed proteins downstream of APOA1 were involved in (Fig. 5).

Subcellular localization analysis. The subcellular localization of the differentially expressed proteins downstream of APOA1 was analyzed. The major subcellular localizations in eukaryotic cells are extracellular, cytoplasm, nucleus, cell membrane, mitochondria, Golgi apparatus, endoplasmic reticulum, peroxisomes, vesicles, cytoskeleton, vesicle membrane, chloroplasts, nucleoplasm, nuclear matrix, and ribosomes. The subcellular localization of the proteins downstream of APOA1 that were differentially expressed proteins between OE + CBP and NC + CBP were analyzed using WoLF PSORT software. The results showed that these proteins were localized to the extracellular matrix (32.8%), nucleus (25%), cytoplasm (15.6%), plasma membrane(15.6%), mitochondria (9.4%) and Golgi apparatus (1.6%) (Fig. 6).

Structural domain annotation and enrichment analysis. The functional structural domains of the differentially expressed proteins downstream of APOA1 between OE + CBP and NC + CBP were analyzed for enrichment using the InterPro database (see Fig. 7).

IPA bioinformatics analysis. We used the keywords JAK STAT, Notch signaling, p38 MAPK signaling, PI3K signaling in B lymphocytes, tumor progression, chemoresistance, recurrence, and metastasis as the input for the IPA bioinformatics analysis. Of the 64 differentially expressed proteins downstream of APOA1, 29 proteins were screened, including 10 upregulated proteins and 19 downregulated proteins, as target proteins for PRM protein identification and quantification.

Quantitative analysis of PRM proteins

Of the 29 screened downstream proteins, 21 were subjected to quantitative PRM protein analysis. Of these 21 proteins, 13 had no statistically significant expression differences between the OE and NC groups but did have statistically significant expression differences between the OE + CBP and NC + CBP groups (Table 2 marked in yellow), suggesting that these 13 proteins, which are downstream factors of APOA1, may be involved in platinum-based chemoresistance in cervical cancer. Literature searches were conducted to find APOA1 downstream proteins and mechanisms affecting resistance to platinum-based chemotherapy in cervical cancer. Our search identified the following: 1) TOP2A, CDKN2A, and APOE, which are involved in tumor growth, recurrence, and metastasis; 2) STAT1, which may be involved in metastasis of tumor through the P38 MAPK signaling pathway; 3) CD81, C3, and RAC1, which may promote tumor progression through the PI3K signaling pathway; and 4) other proteins, such as ALB, AFP, GC, LTF, SOD2, and NDRG1, which are involved in tumor metastasis.

Table 2
PRM identification of APOA1 downstream proteins involved in platinum-based chemotherapy resistance in cervical cancer

No.	Gene name	OE/NC	P value	OE + CBP/NC + CBP	P value
1	CCN1	1.368	0.0011	0.906	0.0252
2	DCTN3	1.084	0.0391	0.809	0.0280
3	**C3**	**1.066**	**0.1338**	**0.646**	**0.0011**
4	**APOE**	**0.863**	**0.2822**	**1.906**	**0.0002**
5	AHSG	1.812	0.0133	0.412	0.0121
6	**ALB**	**1.219**	**0.0926**	**0.468**	**0.0009**
7	**AFP**	**1.097**	**0.1194**	**0.418**	**0.0013**
8	**GC**	**1.040**	**0.1678**	**0.397**	**0.0001**
9	**LTF**	**1.011**	**0.9124**	**0.402**	**0.0001**
10	**SOD2**	**1.020**	**0.8558**	**1.359**	**0.0146**
11	THBS1	0.748	0.0039	0.451	0.0001
12	**TOP2A**	**0.942**	**0.4104**	**0.730**	**0.0079as**
13	MUC1	1.418	0.0153	1.372	0.0089
14	H1-5	2.016	0.0001	0.497	0.0002
15	**STAT1**	**1.009**	**0.8636**	**0.774**	**0.0015**
16	**CDKN2A**	**0.954**	**0.0892**	**0.767**	**0.0061**
17	**CD81**	**0.931**	**0.0978**	**0.692**	**0.0016**
18	B2M	1.375	0.0043	1.305	0.0038
19	**RAC1**	**0.953**	**0.4207**	**0.695**	**0.0156**
20	SLC1A5	0.610	0.0008	0.445	0.0026
21	**NDRG1**	**1.066**	**0.1832**	**1.653**	**0.0006**

Discussion

As the main structural protein of HDL, APOA1 has anti-atherosclerotic, anti-inflammatory, antioxidant, and anti-endotoxic effects [5], and chronic inflammation, oxidative stress, lipids, and cholesterol are associated with tumor development. Several studies have found that serum APOA1 levels are reduced in patients with different malignancies [6–7]. In gynecological tumors, it has been reported that APOA1 levels are significantly downregulated in patients with epithelial ovarian cancer serum, and APOA1 is a

potential tumor marker for epithelial ovarian cancer [8–9]. APOA1 was shown to inhibit tumor development, and low serum levels of APOA1 are associated with poor prognosis. In studies of advanced ovarian cancer, high APOA1 mRNA levels in body fluids were found to be an independent diagnostic factor for clinically longer overall survival (OS) [10].

In a large European prospective study, APOA1 was found to be negatively associated with the risk of colon cancer [11]. In hepatocellular carcinoma, low levels of APOA1 were associated with poorer progression free survival (PFS), thus APOA1 may be a useful predictor of recurrence in hepatocellular carcinoma [12]. In metastatic nasopharyngeal carcinoma, higher serum levels of APOA1 at pre-treatment were associated with higher OS [13]. In breast cancer, low expression of APOA1 predicted a higher risk of breast cancer development and recurrence [14]. The results of some meta-analyses suggest that low levels of APOA1 may be a poor prognostic indicator for various malignancies, including non-small cell lung cancer, gallbladder cancer, and gastric cancer [15].

The mechanism by which APOA1 inhibits tumors is currently unclear. Studies have shown that APOA1 exerts anti-tumor effects mainly by inhibiting tumor cell proliferation and promoting apoptosis [16–17]. APOA1 has been reported to capture circulating tumor cells and promote tumor cell apoptosis by downregulating that MAPK pathway, thereby inhibiting tumor cell proliferation [18]. APOA1 also regulates inflammation signals through the STAT3 signaling pathway and reduces matrix metalloproteinase-9 (MMP-9) levels, which is an important factor that promotes tumor proliferation and metastasis [19]. It has also been reported that a short peptide on APOA1 regulates the phosphorylation of c-Src through the c-Src/ERK signaling pathway, thereby inhibiting tumor growth and angiogenesis [20].

APOA1 is easy to detect clinically and has great value as a marker of tumor prognosis. However, there are few studies on the correlation between APOA1 and tumor chemotherapy. Some studies have reported that APOA1 can be used as a predictive marker for platinum-based chemotherapy resistance in ovarian cancer [21]. In the field of gynecological oncology, proteomic studies have shown that APOA1 is highly expressed in platinum-based chemotherapy-resistant ovarian cancer when compared to the levels in paracancerous tissue. A screen for differentially expressed proteins in serum samples from platinum-resistant and platinum-sensitive patient groups identified APOA1 [22], indicating its association with platinum-based chemoresistance. Cruz et al. [23] searched for proteins related to the proteasomal ubiquitination resistance signaling pathway in platinum-resistant ovarian cancer cells and tissues and found that APOA1 was a significantly upregulated platinum chemoresistance-associated protein and could be used as a predictive marker of platinum chemoresistance in ovarian cancer. However, whether APOA1 is related to chemotherapy in cervical cancer has not yet been reported. In this study, we found that APOA1-overexpressing (OE) and normal control (NC) SiHa and Caski cervical squamous carcinoma cells showed smaller differences in the clone formation rates after administration of chemotherapy compared to the same cells without chemotherapy ($p < 0.05$), indicating that overexpression of APOA1 induced resistance to paclitaxel chemotherapy in cervical cancer cells and reduced the chemotherapy-induced reduction of cell proliferation. In contrast, there were no significant differences in cell proliferation, apoptosis, and migration.

Through bioinformatic analysis and IPA bioanalysis, we found that the factors downstream of APOA1 that are involved in carboplatin chemoresistance in cervical cancer are mainly located in the extracellular matrix and nucleus and may enhance chemoresistance to carboplatin through multiple molecular mechanisms involved in cell composition, cell function, and biological processes. A literature review revealed downstream genes that may be related to chemoresistance: AFP, APOE, B2M, C3, GC, and TOPA2. Our study found seven downstream factors that may be associated with chemoresistance, LTF, SOD2, STAT1, CDKN2A, CD81, RAC1, and NDRG1 and five factors that may be associated with tumor development, CCN1, DCTN3, MUC1, H1-5, and SLC1A5. The specific mechanisms involving these genes need to be further investigated.

We identified and quantitatively validated the proteins downstream of APOA1 by PRM, which indicated that APOA1 may exert its carboplatin chemoresistance effects in cervical squamous carcinoma by 1) promoting tumor growth, recurrence, and metastasis through TOP2A, CDKN2A, and APOE; 2) regulating the P38 MAPK signaling pathway through STAT1 to promote in tumor growth and metastasis; 3) regulating the PI3K signaling pathway through CD81, C3, and RAC1 to promote tumor progression; and 4) promoting metastasis through ALB, AFP, GC, LTF, SOD2, and NDRG1. Our group investigated and validated APOA1-regulated downstream factors involved in the mechanism of platinum-based chemoresistance in cervical squamous carcinoma.

Conclusions

This is a basic research to investigate the mechanism by which apolipoprotein A1 (APOA1) enhances the resistance of cervical squamous carcinoma to platinum-based chemotherapy. Twenty-nine differentially expressed proteins matching cancer-relevant association terms were screened and parallel response monitoring identified 21 as possibly involved in the mechanism of platinum-based chemoresistance. Our analysis suggested that the mechanism may involve numerous regulatory pathways, including promoting tumor growth via the P38 MAPK signaling pathway through STAT1, promoting tumor progression via the PI3K signaling pathway through CD81 and C3, and promoting resistance to platinum-based chemotherapy resistance through TOP2A.

List Of Abbreviatios

APOA1: Apolipoprotein A1

HDL: High-density lipoprotein

CBP: carboplatin

TMT: Tandem Mass Tag

FASP: Filter-aided sample preparation

GO: Gene Ontology

PFS: Progression free survival

MMP-9: Matrix metalloproteinase

Declarations

Ethical Approval and Consent to participate

All procedures performed in studies involving human participants were in accordance with the ethical standards of the institutional and/or national research committee and with the 1964 Helsinki declaration and its later amendments or comparable ethical standards. This study was approved by the Ethic Committee (EC) from the Beijing Obstetrics and Gynecology Hospital, Capital Medical University.

Consent for publication

All authors are consent for publication of this paper on Molecular Cancer.

Availability of supporting data

Certain data types must be deposited in an appropriate public structured data depository (details are available here) and the accession number(s) provided in the manuscript.

Competing Interests

No potential conflict of interest relevant to this article was reported.

Funding

Funding was gratefully received from: Scientific Research Common Program of Beijing Municipal Commission of Education (KM201910025006); Beijing Municipal Science and Technology Commission (grant No. D131100005313009); Beijing Municipal Administration of Hospitals Clinical Medicine Development of Special Funding Support (grant No. ZYLX201705);

Author Contributions

Conceptualization: H.Y., W.Y.M.; Data curation: H.Y., W.Y.M.; Formal analysis: H.Y.; Funding acquisition: H.Y., W.Y.M.; Methodology: H.S.B., L.Y.; Project administration: W.Y.M.; Resources: H.S.B., Z.J.J.; Supervision: W.Y.M.; Writing - original draft: H.Y.; Writing - review & editing: W.Y.M.

Acknowledgements

We are grateful to all the reviewers and editors who provided comments that substantially improved the manuscript.

Authors' information

Not applicable.

References

1. Koh WJ, Abu-Rustum NR, Bean S, et al. Cervical cancer, Version 3.2019, NCCN Clinical Practice Guidelines in Oncology [J]. J Natl Compr Canc Netw. 2019;17(1):64–84.
2. Zamanian-Daryoush M, DiDonato JA. Apolipoprotein A-I and cancer [J]. Front Pharmacol. 2015;6:265.
3. Han SB, He Y, Wu YM. Establishment of stable cervical cancer cell line overexpressing apolipoprotein A1 mediated by lentivirus [J]. Chinese J of Medicine,2020,42(2):172–174.
4. He Y, Han SB, Geng YN, et al. Quantitative analysis of proteins related to chemoresistance to paclitaxel and carboplatin in human SiHa cervical cancer cells via iTRAQ [J]. J Gynecol Oncol. 2020;31:e28.
5. Gordon SM, Hofmann S, Askew DS, et al. High density lipoprotein: it's not just about lipid transport anymore [J]. Trends Endocrinol Metab. 2011;22(1):9–15.
6. Lei T, Zhao X, Jin S, et al. Discovery of potential bladder cancer biomarkers by comparative urine proteomics and analysis [J]. Clin Genitourin Cancer. 2013;11(1):56–62.
7. Liu X, Zheng W, Wang W, et al. A new panel of pancreatic cancer biomarkers discovered using a mass spectrometry-based pipeline [J]. Br J Cancer. 2017;117(12):1846–54.
8. Wegdam W, Argmann CA, Kramer G, et al. Label-free LC-MSe in tissue and serum reveals protein networks underlying differences between benign and malignant serous ovarian tumors [J]. PLoS One. 2014;9(9):e108046.
9. Clarke CH, Yip C, Badgwell D, et al. Proteomic biomarkers apolipoprotein A1, truncated transthyretin and connective tissue activating protein III enhance the sensitivity of CA125 for detecting early stage epithelial ovarian cancer [J]. Gynecol Oncol. 2011;122(3):548–53.
10. Tuft SH, Nymoen DA, Hetland FT, et al. APOA1 mRNA expression in ovarian serous carcinoma effusions is a marker of longer survival [J]. Am J Clin Pathol. 2014;142(1):51–7.
11. van Duijnhoven FJ, Bueno-De-Mesquita HB, Calligaro M, et al. Blood lipid and lipoprotein concentrations and colorectal cancer risk in the European Prospective Investigation into Cancer and Nutrition [J]. Gut. 2011;60(8):1094–102.
12. Ni XC, Yi Y, Fu YP, et al. Role of lipids and apolipoproteins in predicting the prognosis of hepatocellular carcinoma after resection [J]. Onco Targets Ther. 2020;13:12867–80.
13. Jiang R, Yang ZH, Luo DH, et al. Elevated apolipoprotein A-I levels are associated with favorable prognosis in metastatic nasopharyngeal carcinoma [J]. Med Oncol. 2014;31(8):80.
14. Budczies J, Denkert C, Muller BM, et al. Remodeling of central metabolism in invasive breast cancer compared to normal breast tissue - a GC-TOFMS based metabolomics study [J]. BMC Genom.

2012;13:334.

15. Zhang Y, Yang X. Prognostic significance of pretreatment apolipoprotein A-I as a noninvasive biomarker in cancer survivors: A meta-analysis [J]. Dis Markers, 2018, 2018:1034037.
16. Gautier EL, Yvan-Charvet L. HDL and its transporters ABCA1 and ABCG1 regulate innate immunity and hematopoietic stem cell proliferation [J]. Med Sci (Paris). 2011;27(1):9–11.
17. Castaing-Berthou A, Malet N, Radojkovic C, et al. PI3Kbeta plays a key role in apolipoprotein A-I-induced endothelial cell proliferation through activation of the Ecto-F1-ATPase/P2Y1 receptors [J]. Cell Physiol Biochem. 2017;42(2):579–93.
18. Mao D, Che J, Han S, et al. RNAi-mediated knockdown of the CLN3 gene inhibits proliferation and promotes apoptosis in drug-resistant ovarian cancer cells [J]. Mol Med Rep. 2015;12(5):6635–41.
19. Jia ZH, Jia Y, Guo FJ, et al. Phosphorylation of STAT3 at Tyr705 regulates MMP-9 production in epithelial ovarian cancer[J]. PLoS One. 2017;12(8):e183622.
20. Yi ZF, Cho SG, Zhao H, et al. A novel peptide from human apolipoprotein(a) inhibits angiogenesis and tumor growth by targeting c-Src phosphorylation in VEGF-induced human umbilical endothelial cells [J]. Int J Cancer. 2009;124(4):843–52.
21. Cruz IN, Coley HM, Kramer HB, et al. Proteomics analysis of ovarian cancer cell lines and tissues reveals drug resistance-associated proteins [J]. Cancer Genom Proteom. 2017;14(1):35–51.
22. Wu WJ, Wang Q, Zhang W, et al. Screening and clinical value of differentially expressed proteins related to platinum resistance in serum of patients with epithelial ovarian cancer [J]. Chin J of Obstet Gynecol. 2016;51(7):515–23.
23. Cruz IN, Coley HM, Kramer HB, et al. Proteomics analysis of ovarian cancer cell lines and tissues reveals drug resistance-associated proteins [J]. Cancer Genomics Proteomics. 2017;14(1):35–51.

Figures

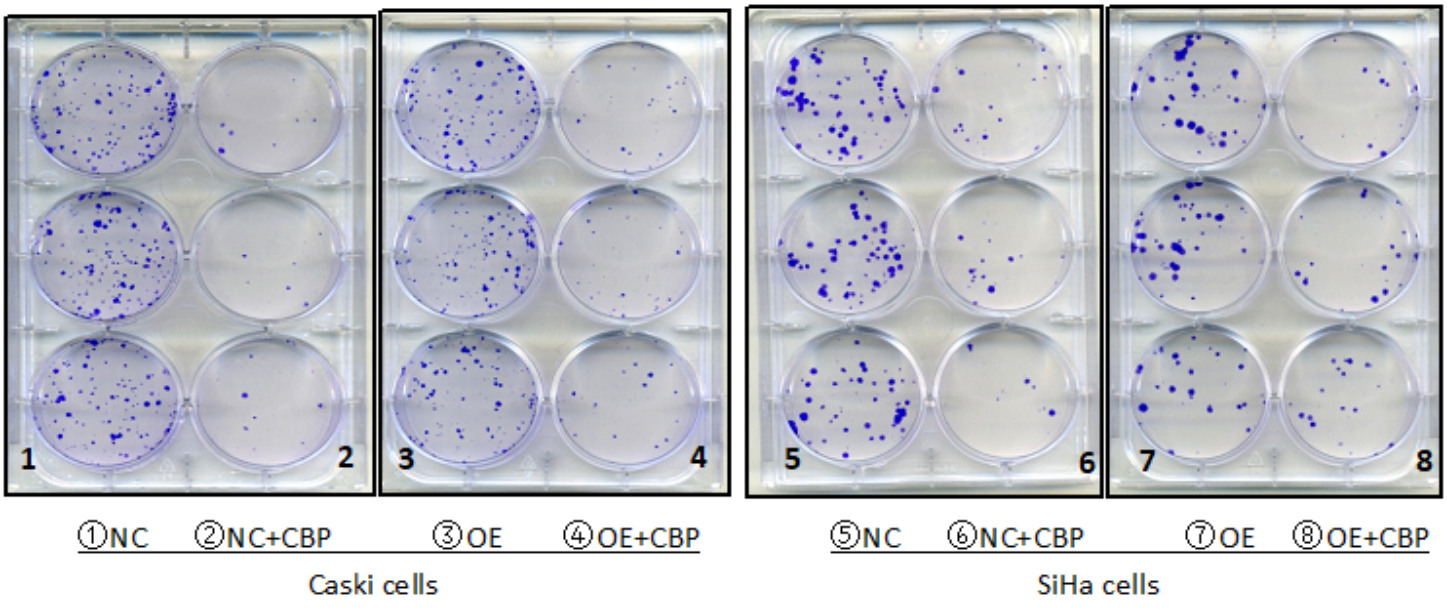

Figure 1

Clone formation assay of APOA1-overexpressing SiHa and Caski cells NC: SiHa or Caski cells treated with vehicle for 48 h; OE: SiHa or Caski APOA1-overexpressing cells treated with vehicle for 48 h; NC+CBP: SiHa or Caski cells treated with CBP for 48 h, OE+CBP: SiHa or Caski APOA1-overexpressing cells treated with CBP for 48 h

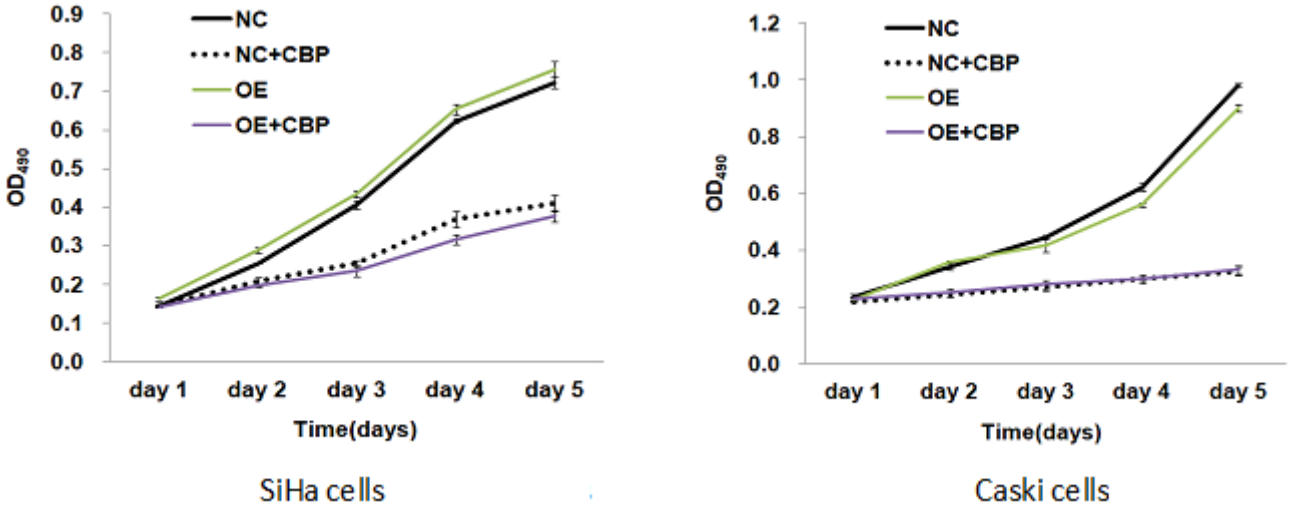

Figure 2

MTT assay to assess the effect of APOA1 overexpression on the proliferation of SiHa and Caski cells

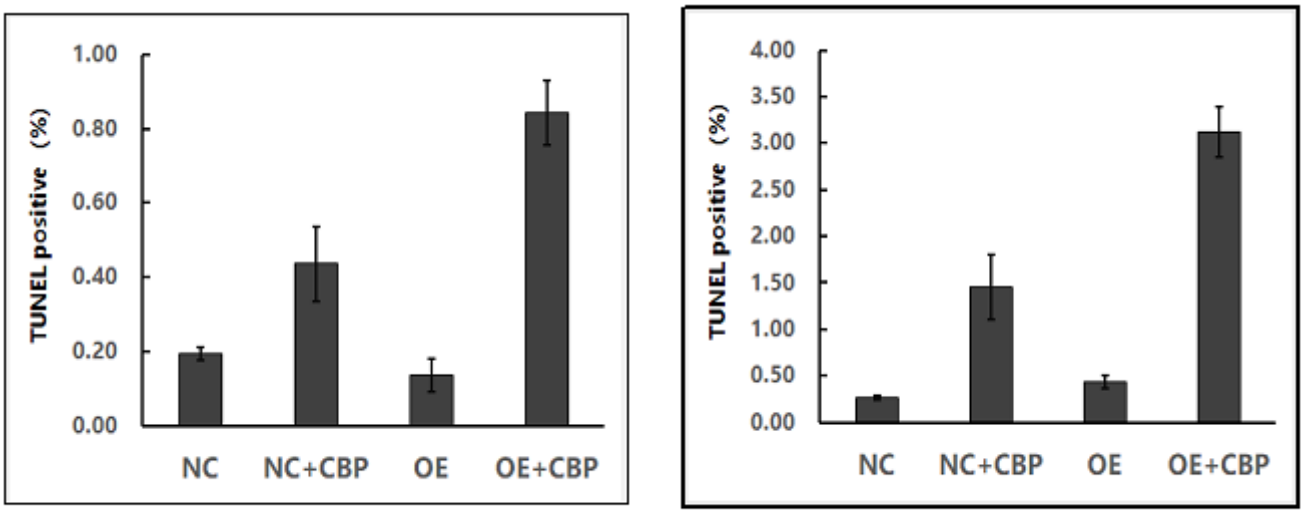

Figure 3

TUNEL assay to detect the effect of APOA1 overexpression on apoptosis of SiHa/Caski cells with and without CBP NC: SiHa or Caski cells treated with vehicle for 48 h; OE: SiHa or Caski APOA1-overexpressing cells treated with vehicle for 48 h; NC+CBP: SiHa or Caski cells treated with CBP for 48 h, OE+CBP: SiHa or Caski APOA1-overexpressing cells treated with CBP for 48 h

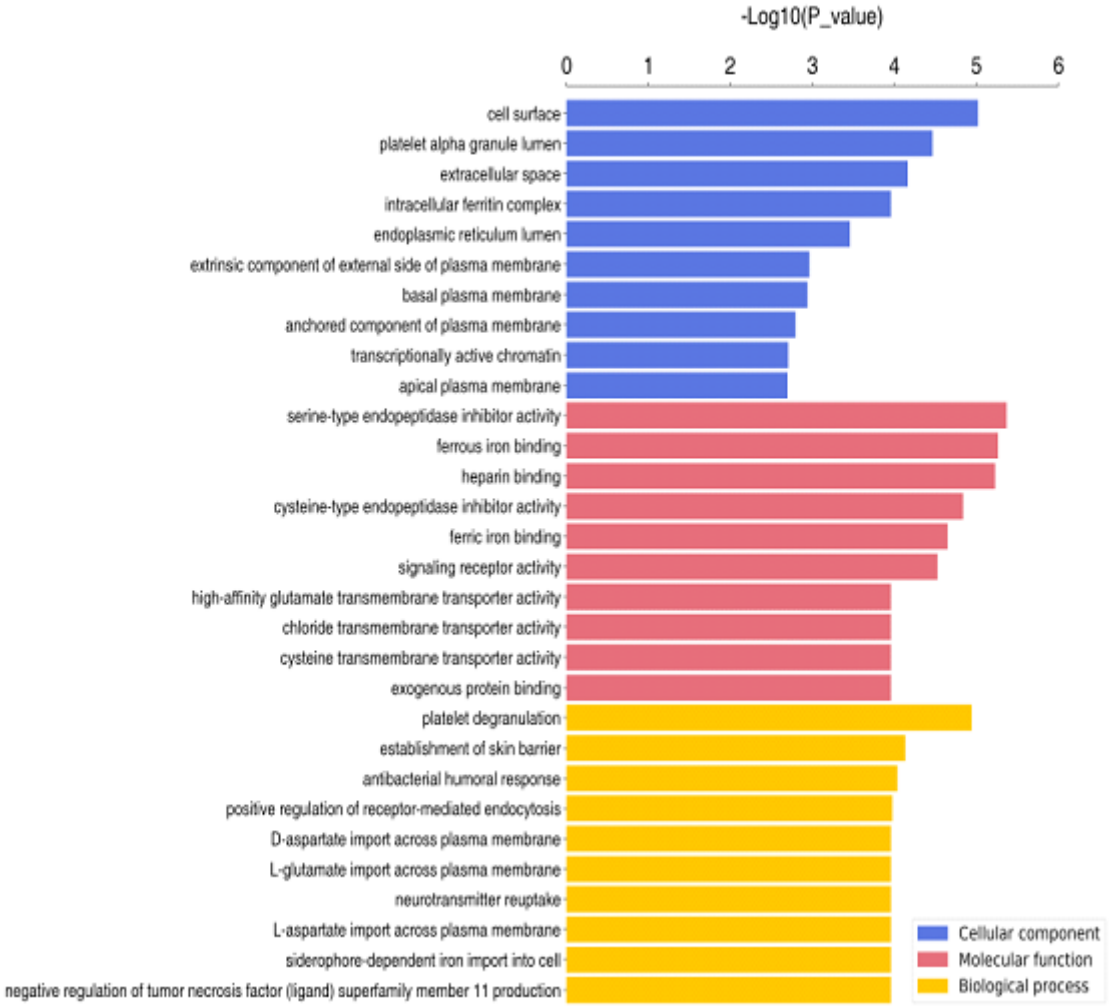

Figure 4

GO enrichment analysis of the differentially expressed proteins in cells overexpressing APOA1 and normal control cells treated with carboplatin

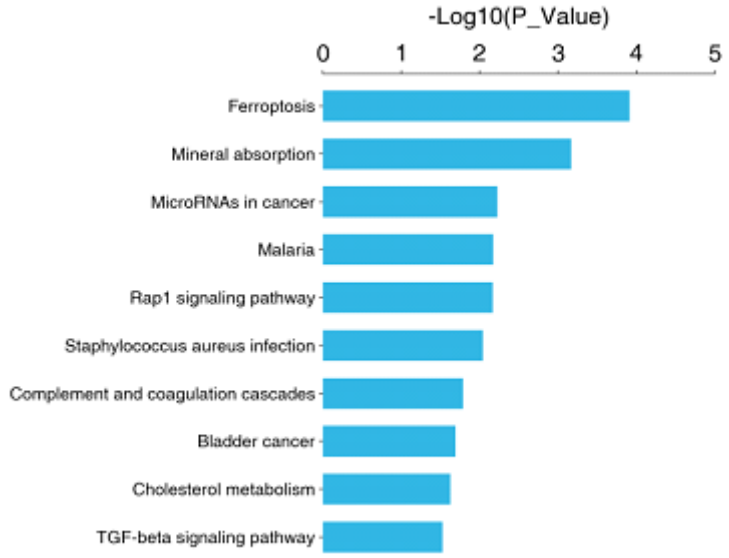

Figure 5

KEGG pathway enrichment analysis of the differentially expressed proteins in cells overexpressing APOA1 and normal control cells treated with carboplatin

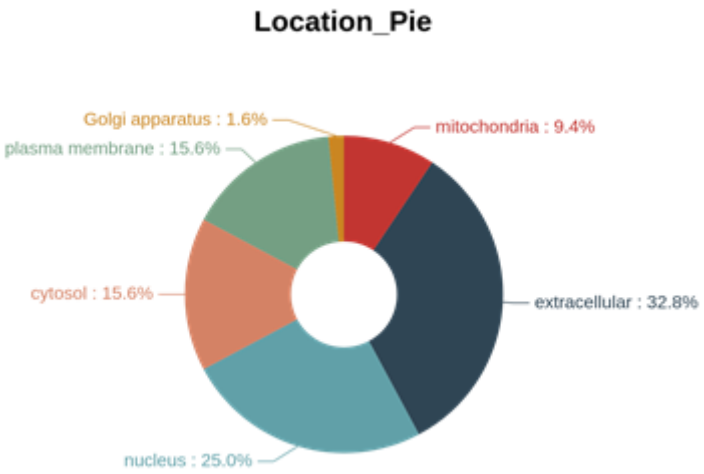

Figure 6

Subcellular localization of the differentially expressed proteins in cells overexpressing APOA1 and normal control cells treated with carboplatin

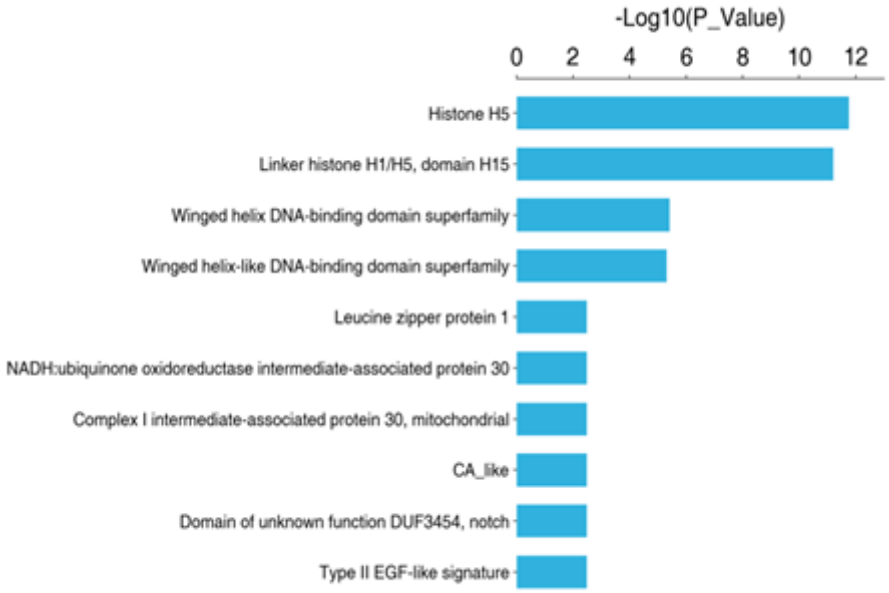

Figure 7

Structural domain annotation and enrichment analysis in cells overexpressing APOA1 and normal control cells treated with carboplatin